

## Characteristics and Adsorption Test of Activated Carbon from Indonesian Bituminous Coal

Esthi Kusdarini<sup>1\*</sup>, Agus Budiarto<sup>2</sup>

<sup>1</sup> Mining Engineering Department, Faculty of Mineral and Marine Technology, Institut Teknologi Adhi Tama Surabaya, Jl. Arief Rachman Hakim 100 Surabaya 60117, Indonesia

<sup>2</sup> Chemical Engineering Department, Faculty of Industrial Technology, Institut Teknologi Adhi Tama Surabaya, Jl. Arief Rachman Hakim 100 Surabaya 60117, Indonesia

\* Corresponding author's e-mail: esti@itats.ac.id

### ABSTRACT

The fast-growing batik industry in Indonesia raises the problem of the waste containing chromium. One method to remove chromium is by the adsorption process using activated carbon. Activated carbon can be made from coal. This commodity is a mining mineral the availability of which is still abundant in Indonesia. This study aimed to obtain: 1) the best concentration of activator and activation temperature in the manufacture of activated carbon; 2) characteristics of activated carbon (moisture content, volatile matter content, ash content, fixed carbon content, iodine number, specific surface area, pore-volume, pore surface area, pore radius, and SEM photos); 3) % activated carbon removal for chromium and maximum adsorption capacity for chromium; 4) Freundlich and Langmuir isotherm adsorption equation of activated carbon to chromium. The manufacture of activated carbon was carried out by a carbonization process followed by a chemical and physical activation processes. The chemical activator was ammonium phosphate with doses of 74.5 g/L, 149 g/L, 223.5 g/L, and 298 g/L. Meanwhile, physical activation was carried out at 848 K, 948 K, 1048 K, and 1148 K. The next step was to test the adsorption capacity of activated carbon on artificial batik waste containing chromium. The results showed that: 1) activator concentration did not significantly affect the characteristics of activated carbon. Meanwhile, the optimal activation temperature is at a temperature of 1048 K and 1148 K, which can produce the activated carbon that meets the requirements of activated carbon of the Indonesian National Standard 06-3730-1995 with the following contents: air content 0.16–0.81%; volatile matter 14.62–19.31%; ash 6.48–9.97%; fixed carbon 70.60–75.79%; iodine number 1243.13–1258.65%; specific surface area 31.930 m<sup>2</sup>/g; activated carbon pore volume 0.011 cc/g; pore surface area 8.905 m<sup>2</sup>/g; activated carbon pore radius 30.614; 3) the proportion of activated carbon removal for chromium is 37–53% and the maximum adsorption capacity for chromium is 52 mg/g; 4) the Freundlich equation test resulted in a constant  $R^2$  of 0.5126,  $n$  2.4870,  $K_F$  8.8818 mg/g, while the Langmuir equation test resulted in a constant  $R^2$  of 0.8897,  $b$  -0.0075 L/mg,  $q_m$  -90.0901 mg/g.

**Keywords:** ammonium phosphate, coal, batik waste, activated carbon, chromium.

### INTRODUCTION

Batik is one of the products of the Indonesian nation's art and culture that is in great demand by people, both the Indonesian people themselves and tourists from other countries. However, the proliferation of the batik industry increases the pollution of water bodies due to its waste. Batik waste contains chromium due to the use of chemical dyes in the dyeing and washing process

(Mahmudi et al., 2020; Wirosedarmo et al., 2020). If the waste containing chromium is discharged directly into water bodies, it causes river water pollution and endangers the lives of living things. Chromium ions in water were detected as Cr(III) and Cr(VI). Cr(VI) is a toxic contaminant. This metal can accumulate in the human body through the  $\text{CrO}_4^{2-}$  and  $\text{Cr}_2\text{O}_7^{2-}$  compounds soluble in water and cause toxic effects on biological systems (Dhivya et al., 2019; Gong et al., 2017;

W. Liu et al., 2019). Chromium metal contamination in water bodies can endanger the health of living things exposed to it and the sustainability of the environment (A. Yáñez-Varela et al., 2018). The maximum allowable chromium content in water is 0.05 mg/L (Effendi, 2003). Therefore, the chromium content in batik waste must be minimized before discharge into water bodies.

There are several methods to minimize the chromium content in batik waste, including using the filtration method (Kusdarini et al., 2021; Kusdarini et al., 2020), ion exchange (Kusdarini and Budianto, 2018; Kusdarini et al., 2018, 2021), and adsorption (Budianto et al., 2021; Budianto et al., 2019; Budianto et al., 2019; Kusdarini et al., 2017). The adsorption process with activated carbon is cheap and easy to operate. Activated carbon raw materials are organic materials. One of the raw materials for activated carbon, abundantly available in Indonesia, is coal.

Several studies have been carried out to make activated carbon from coal. Activated carbon made from low-grade bituminous coal has a maximum specific surface area of 86.213 m<sup>2</sup>/g and an iodine value of 1238.544 mg/g (Kusdarini et al., 2017). Meanwhile, activated carbon from lignite coal has an iodine value of 1288.8 m<sup>2</sup>/g (Sulistyah and Astuti, 2021). In addition to low and medium-grade coal, several studies have also made activated carbon from high-grade coal. The activated carbon from anthracite coal has a maximum adsorption capacity of 19.31 mmol/g CH<sub>4</sub> gas (X. Liu et al., 2022). This research has successfully produced the activated carbon that partially fulfills the parameter requirements of SNI 06-3730-1995. However, it does not meet the standards for several other parameters. Therefore, this research refined the previous study with the novelty of using ammonium phosphate for chemical activation and high temperature for physical activation, namely 848–1148 K.

## MATERIALS AND METHODS

### Materials and tools

The materials used in this research are coal, (NH<sub>4</sub>)<sub>3</sub>PO<sub>4</sub>, NaOH, starch, iodine, Na<sub>2</sub>SO<sub>3</sub>, H<sub>2</sub>CrO<sub>4</sub>, and aquadest. In turn, the tools used are a hammer, grinder, analytical balance, dropper, measuring flask, clamp, filter paper, burette,

furnace, beaker glass, aluminum foil, funnel, measuring cup, and Erlenmeyer flask.

### Coal testing

Determination of parameters and types of coal raw materials was carried out using proximate analysis, namely testing water content (ASTM D-3173-92), volatile matter content (BS-1016), and ash content (ASTM D-3174-98). The fixed carbon content was calculated based on the formula:

$$\text{water content} + \text{volatile matter content} + \text{ash content} + \text{fixed carbon content} = 100\% \quad (1)$$

### Activated carbon manufacture

Preparing raw materials before processing included: 1) grinding coal, 2) sifting with a 60 mesh sieve, 3) separating coal granules with a size of < 60 mesh to be used as raw material for activated carbon. In turn, the manufacture of activated carbon included: 1) dehydration, which is drying coal in the sun for 2 days, 2) carbonization, which is heating coal at a temperature of 550 °C for 2 hours; 3) chemical activation, namely soaking charcoal in ammonium phosphate activator at a dose of 74.5 g/L, 149 g/L, 223.5 g/L, and 298 g/L, neutralization of the charcoal using 0.1 M sodium hydroxide and aquadest, separation of the charcoal from the neutralizing solution with a filter paper; 4) physical activation, namely heating coal charcoal at temperatures of 848 K, 948 K, 1048 K, and 1148 K; 5) store activated carbon in aluminum foil for analysis.

### Activated carbon analysis

Activated carbon analysis includes: 1) Proximate analysis (same procedure as for coal raw material proximate analysis), 2) Iodine number analysis (ASTM D-4607-94), 3) BET, 4) SEM-EDX

### Testing the ability to remove chromium solution by activated carbon

Tests were carried out on Cr<sup>6+</sup> ions contained in chromic acid solution. Then, 1 g of activated carbon was placed into 1 L of chromic acid solution at a dose of 120 mg/L (sample E), 105 mg/L (sample F), 90 mg/L (sample G), 75 mg/L (sample H), and 60 mg/L (sample I), stirred at 450 rpm for

3.5 hours. Furthermore, analysis of the chromium content in the chromic acid solution was carried out before ( $C_o$ ) and after contact with activated carbon ( $C_e$ ) (SNI 6989.71:2009). The ability of activated carbon to remove chromium in water is expressed in % chromium removal (Equation 2).

$$\% \text{ removal chromium } (Cr) = \frac{C_o - C_e}{C_o} \times 100\% \quad (2)$$

### Isotherm adsorption test with Freundlich and Langmuir equation

Freundlich assumed heterogeneous surfaces with different adsorption energies. According to Equation 3,  $K_F$  and  $n$  are Freundlich constants determining adsorption capacity and intensity. This constant can be obtained from the intercept and slope of the log diagram  $q_e$  versus  $C_e$  (Nowruzi et al., 2020).

$$q_e = K_F C_e^{\frac{1}{n}} \quad (3)$$

Where  $q_e$  notation is the equilibrium capacity of  $Cr^{6+}$  ions, namely the number of  $Cr^{6+}$  ions adsorbed per unit mass of activated carbon (mg/g),  $C_e$  is the equilibrium concentration of  $Cr^{6+}$  ions in solution after activated carbon has been adsorbed (mg/L),  $K_F$  and  $n$  are empirical constants (Basu et al., 2018; Kusdarini et al., 2018, 2021). The  $K_F$  and  $n$  constants can be found by Equation 4.

$$\log q_e = \log K_F + \frac{1}{n} \log C_e \quad (4)$$

Determining the  $K_F$  and  $n$  constants in the Freundlich equation was carried out by plotting  $\log q_e$  vs  $\log C_e$  as in Equation 4. The Langmuir isothermal adsorption equation is present in Equation 5.

$$\frac{C_e}{q_e} = \frac{C_e}{q_m} + \frac{1}{b q_m} \quad (5)$$

Where  $C_e$  (mg/L) is the equilibrium concentration of  $Cr^{6+}$  ions in the solution after activated carbon has been adsorbed,  $q_e$  is the capacity for  $Cr^{6+}$  ion equilibrium, namely the weight of  $Cr^{6+}$  ions adsorbed per unit weight of activated carbon (mg/g),  $b$  (L/mg) and  $q_m$  (mg/g) is the Langmuir constant which corresponds to the adsorption energy and the maximum adsorption capacity respectively and is determined from the intercept and slope diagram  $\frac{C_e}{q_e}$  versus  $C_e$ .

## RESULTS

### Characteristics of coal and activated carbon

The results of the proximate coal analysis show that water content is 4.3%, volatile matter content is 14.3%, ash content is 8.4%, and fixed carbon content is 73.1%, so it belongs to the bituminous coal group (Hessley et al., 1986; Kirk and Othmer, 1979). Meanwhile, the results of testing parameters for activated carbon made with variable concentration of activator and activation temperature are shown in Figure 1 (water content), Figure 2 (ash content), Figure 3 (volatile matter), Figure 4 (fixed carbon), and Figure 5 (iodine numbers).

### Water content parameter

The moisture content of the activated carbon sample is 0.16–7.73%, as shown in Figure 1. The water content meets the SNI standard 06-3730-1995 (BSN, 1995). The activator concentration  $(NH_4)_3PO_4$  did not affect the water content. The water content of activated carbon, which was activated at a temperature of 1048 K and 1148 K, experienced a sharp difference compared to the activation temperature of 848 K and 948 K. At an activation temperature of 848 K, the water content of activated carbon was smaller (3.43–3.61%) than the activated carbon made from bituminous coal, which is activated using the activator  $H_3PO_4$  and  $NH_4HCO_3$  at an activation temperature of 873 K, reaching 6.6–8% (Kusdarini et al., 2017), and activated carbon made from young coconut coir and shells which is activated using NaOH activator at an activation temperature of 873 K, reaching 2–18% (Budianto et al., 2021). At an activation temperature of 1148 K, the water content of activated carbon is smaller (0.37–0.81%) than the activated carbon made from peat soil and coal, which is activated using the activator  $H_3PO_4$ ,  $H_2SO_4$ , and  $ZnCl_2$  at an activation temperature of 1173 K, amounting to 4.1–4.3% (Budihardjo et al., 2021). Meanwhile, at the activation temperature of 948 K, the water content of activated carbon is higher (6.34–7.73%) than the activated carbon made from empty palm oil bunches waste, which is activated using an  $H_3PO_4$  activator at an activation temperature of 973 K, equal to 3%. (Budianto et al., 2021). The water content of the product is higher than the water content of activated carbon from mangrove charcoal with a

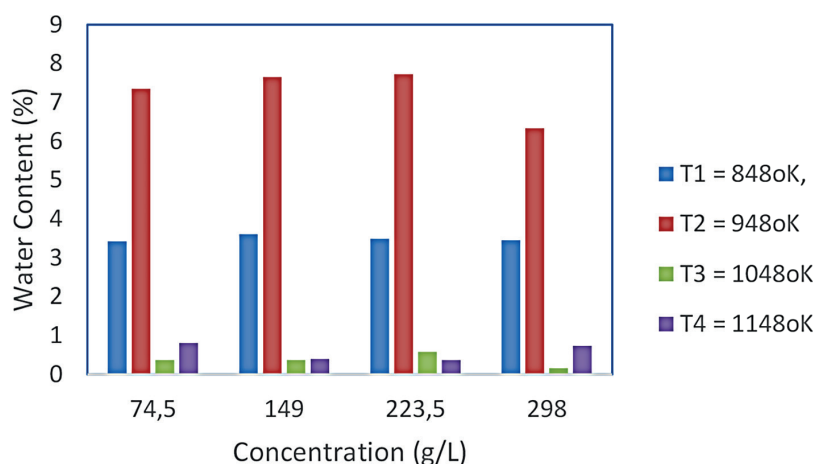


**Figure 1.** Diagram of the percentage of activated carbon water content with variable concentration of chemical activator and physical activation temperature

phosphoric acid activator (Budianto et al., 2019). The water content of activated carbon at an activation temperature of 1048–1148 K is almost the same (0.16–0.81%) compared to the activated carbon made from mangrove charcoal which is activated using phosphoric acid at an activation temperature of 923–998 K, amounting to 0.11–0.38%. (Budianto et al., 2019).

#### Ash content parameter

The ash content parameter of activated carbon is volatile, i.e., 6.48–25.45%. The ash content meets SNI standards if it amounts to a maximum of 10%. This condition occurs in the activation process with a physical activation temperature of 1048–1148 K, which is 6.48–9.97% (BSN, 1995).

Figure 2 shows that the activation temperature affects the ash content, while the ammonium phosphate concentration does not show a trend towards the ash content. Parameters of the ash content of activated carbon are not much different from activated carbon from low-grade bituminous coal and mangrove charcoal (Budianto et al., 2019; Kusdarini et al., 2017).

#### Volatile matter content parameter

The parameters of the volatile matter content of activated carbon are 14.38–26.74%, or 94% of the activated carbon samples made that meet the SNI standard, which is a maximum of 25% (Figure 3) (BSN, 1995). This value is lower than the volatile matter of the activated carbon made

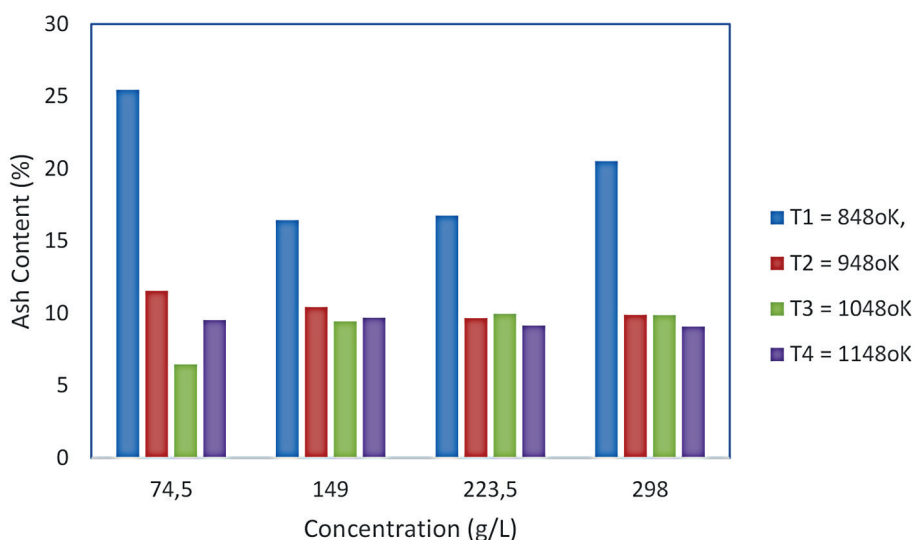


**Figure 2.** Diagram of the percentage of ash content of activated carbon with variable concentration of chemical activator and physical activation temperature

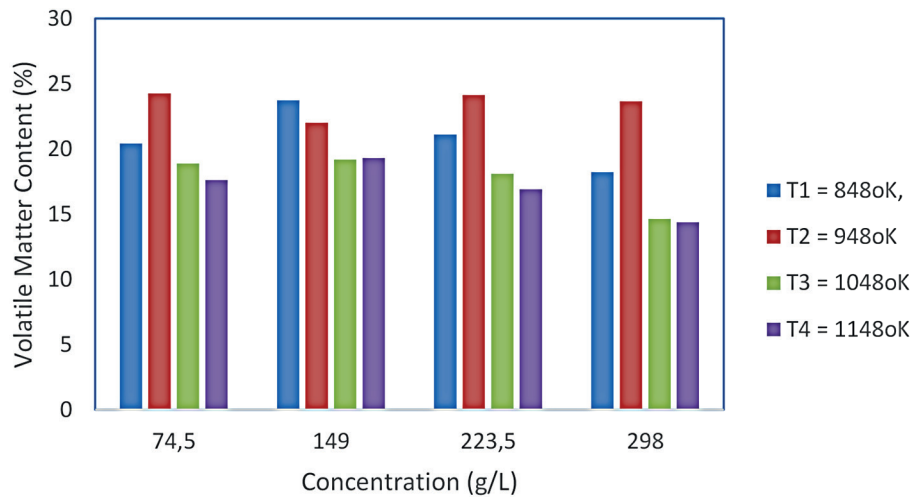


**Figure 3.** Diagram of the percentage of the volatile matter content of activated carbon with variable concentration of chemical activator and physical activation temperature

from low-grade bituminous coal and the activated carbon from young coconut coir and shells (Budianto et al., 2021; Kusdarini et al., 2017). The volatile matter of activated carbon is almost the same as that of the activated carbon made from mangrove charcoal (Budianto et al., 2019). Furthermore, the volatile matter value of activated carbon is higher than that of the activated carbon made from empty palm oil bunches waste (Budianto et al., 2021).

#### Fixed carbon content parameter

The fixed carbon content of activated carbon is 50.70–75.79%. The results showed that the concentration of the chemical activator did not significantly affect the fixed carbon content

of activated carbon. In the temperature range of 1048 K and 1148 K, as shown in Figure 4, the fixed carbon of the product increased sharply. Fixed carbon in the product meets SNI standards at these two temperatures, which is at least 65% (BSN, 1995). Fixed carbon activated carbon from this research is higher than the activated carbon from low-grade bituminous coal (Kusdarini et al., 2017). However, fixed carbon activated carbon is lower than the fixed carbon made from mangrove charcoal and empty palm oil bunches waste (Budianto et al., 2021; Budianto et al., 2019).

#### Iodin number parameter

The parameter iodine number for activated carbon is 1248–1259 mg/g or has met the SNI

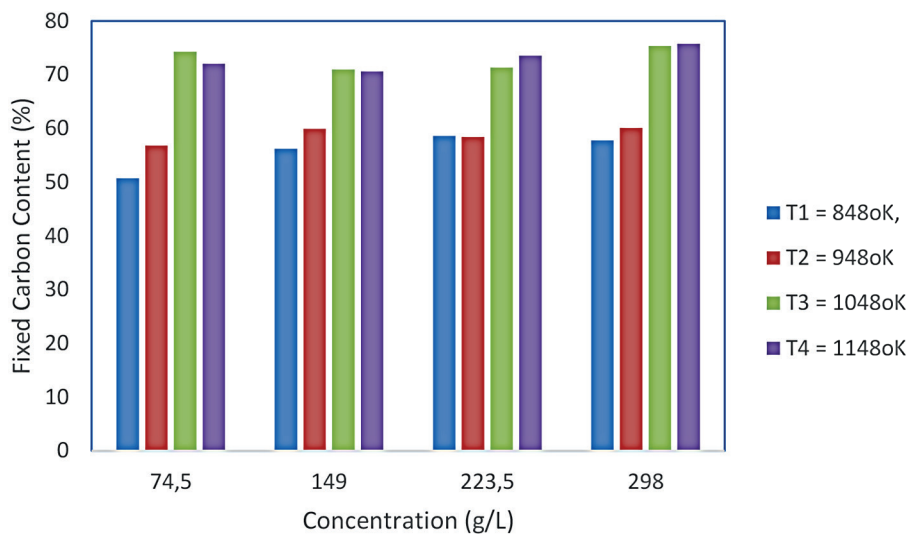


**Figure 4.** Diagram of the percentage of the fixed carbon of activated carbon with variable concentration of chemical activator and physical activation temperature

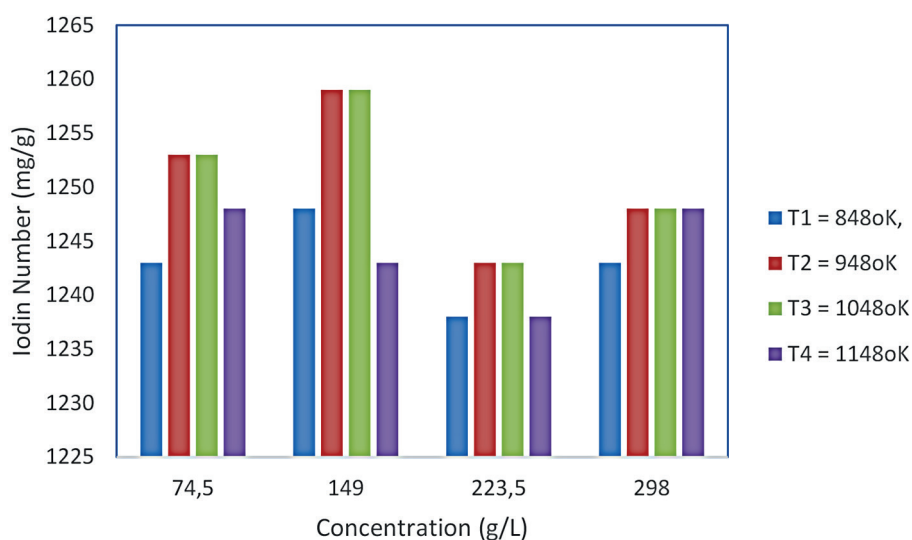


**Figure 5.** Diagram of activated carbon iodine number with variable concentration of chemical activator and physical activation temperature

standard, which is at least 750 mg/g as shown in Figure 5 (BSN, 1995). This iodine number is higher than the iodine number for the activated carbon from mangrove charcoal, low-grade bituminous coal, and empty palm oil bunches waste (Budianto et al., 2021; Budianto et al., 2019; Kusdarini et al., 2017).

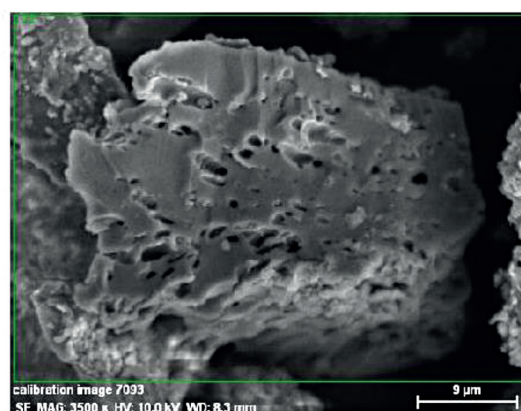
#### Analisa brunauer emmett teller (BET)

The morphological characteristics of activated carbon showed that the specific surface area of activated carbon was 31.930 m<sup>2</sup>/g, the pore volume of activated carbon was 0.011 cc/g, and the pore surface area was 8.905 m<sup>2</sup>/g, and the pore radius was 30.614. The morphological characteristics of activated carbon are better than the activated carbon from the bark of salak, namely a specific surface area of 15.75 m<sup>2</sup>/g and a pore volume of 0.0027 cc/g (Fatimah et al., 2021). The surface area of activated carbon from bituminous coal is also larger than the activated carbon from anthracite coal which is activated with a 50% KOH solution at a temperature of 700 °C with an N<sub>2</sub> gas flow of 29.00 m<sup>2</sup>/g (Song et al., 2020). In addition, the morphological characteristics of activated carbon from the research are also better than the ZwitAd adsorber made of acrylic coating material, bentonite, distilled water, surfactant (epichlorohydrin-dimethyl amine) with a specific surface area of 2.75 m<sup>2</sup>/g and a pore volume of 0.018 cc/g (Azha and Ismail, 2021).

#### SEM-EDX

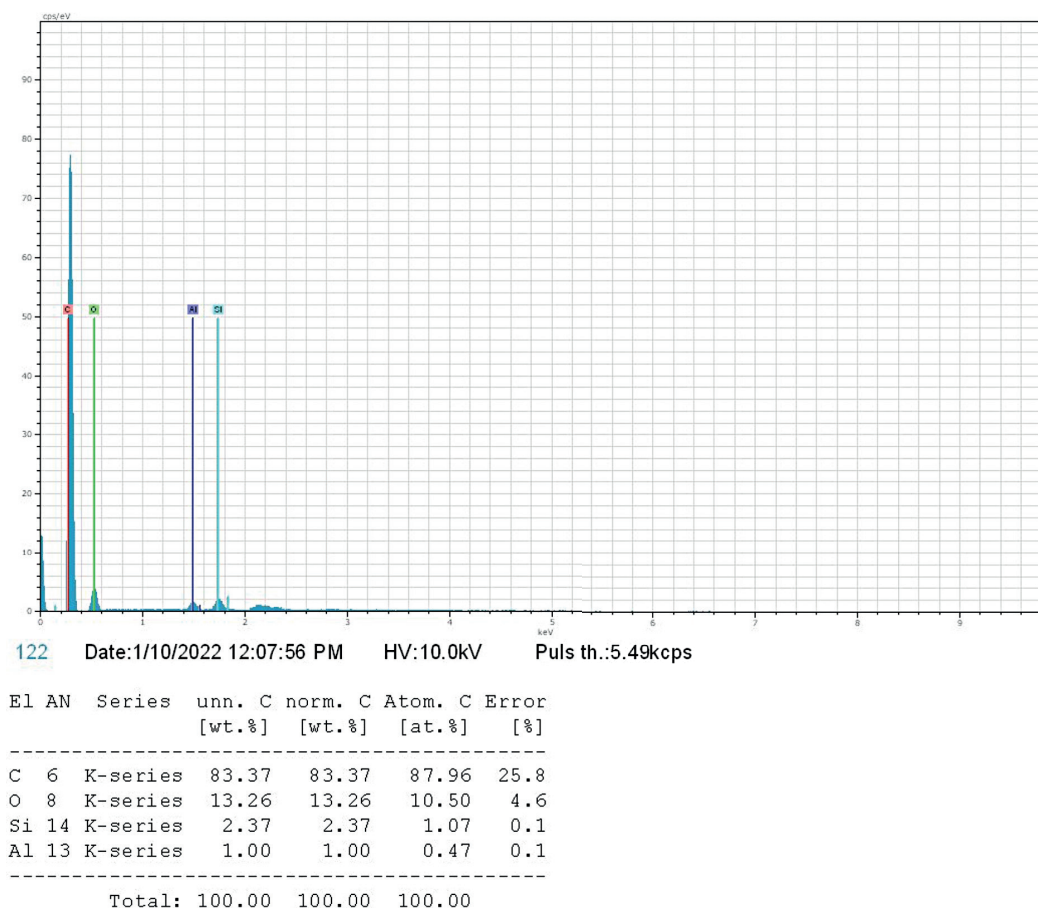
The surface morphology and elemental composition of carbonized coal are presented in Figures 6 and 7. In comparison, the surface morphology and elemental composition of activated carbon after chemical and physical activation are presented in Figures 8 and 9.

Figure 6 is a coal surface carbonization process. The substance has a relatively smooth surface area, irregular block structure, and no apparent pore structure. This condition is due to the relatively low carbonization process temperature for the pyrolysis temperature (Ming-Ming Fu et al., 2019).



calibration image 7093Date:1/10/2022  
12:06:25 PMImage size:512 x  
384Mag:3500xHV:10.0kV

**Figure 6.** Coal surface view after carbonization process (512 x) with SEM-EDX equipment



**Figure 7.** Composition of elements C, O, Si, and Al in carbon before activation

SEM photos show that after the carbon after chemical and physical activation, as shown in Figure 9, it has more comprehensive, numerous pores and a more apparent pore structure than carbonized carbon.

### Removal chromium

Initial ( $C_0$ ) and late ( $C_e$ ) Cr(VI) concentrations and the percentage of chromium removal in several concentrations of Cr in solution after contact with activated carbon are presented in Table 1. The % Cr removal of 37–53%. Each volume of 1 L was contacted with 1 g of activated carbon until equilibrium was reached. From Table 1, it can be seen that the maximum adsorption capacity of activated carbon on Cr in sample B was 52 mg/g.

### Adsorption isotherm

The isotherm study describes the behavior of the adsorbent and states the relationship between the amount of adsorbate adsorbed by the

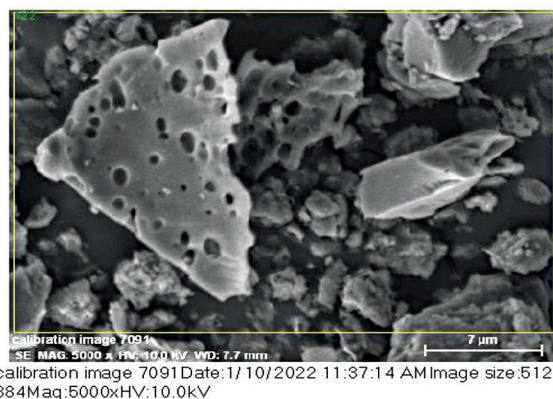


**Figure 8.** The appearance of the carbon surface after chemical and physical activation (512 x) using the SEM-EDX apparatus

**Table 1.** Percentage of chromium removal at various concentrations

Sample	E	F	G	H	I
$C_0$ (mg/L)	120	105	90	75	60
$C_e$ (mg/L)	76	53	45	35	29
$C_0 - C_e$ (mg/L)	44	52	45	40	31
% removal Cr	37	50	50	53	52

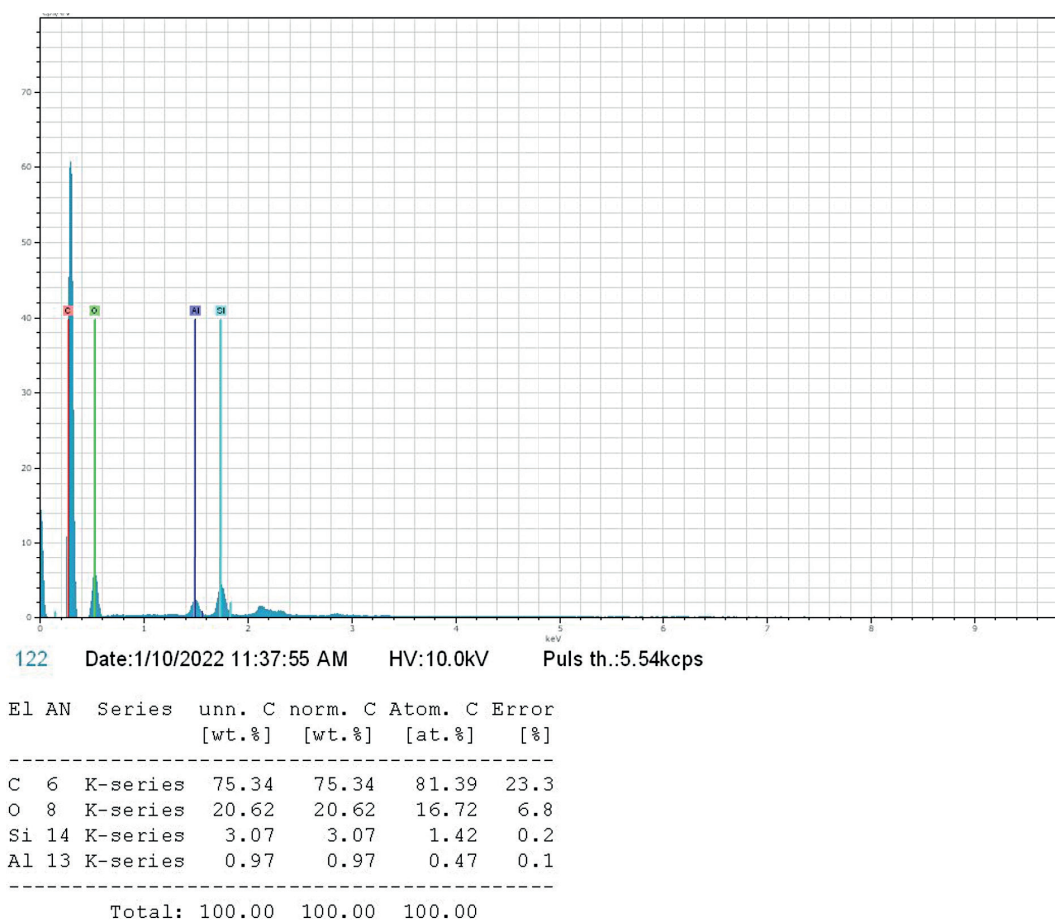


Figure 9. Composition of elements C, O, Si, and Al in carbon after activation

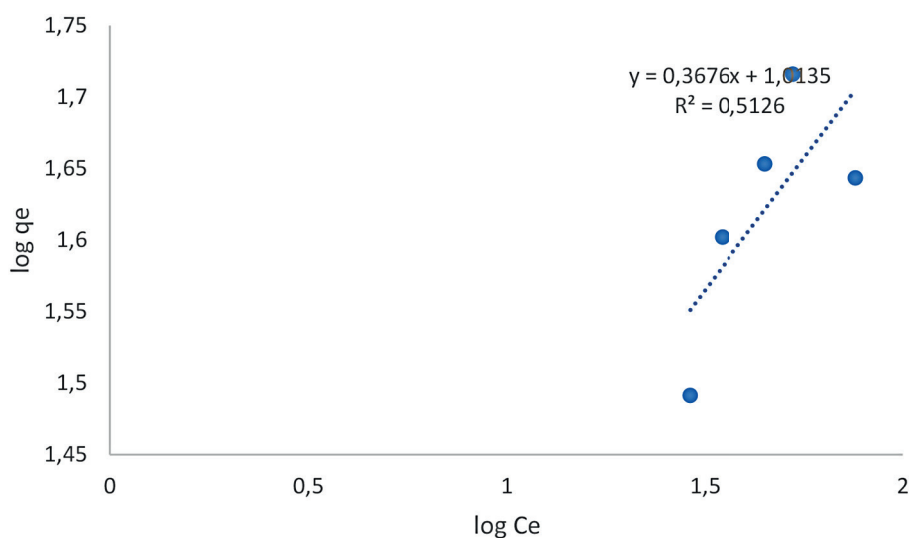
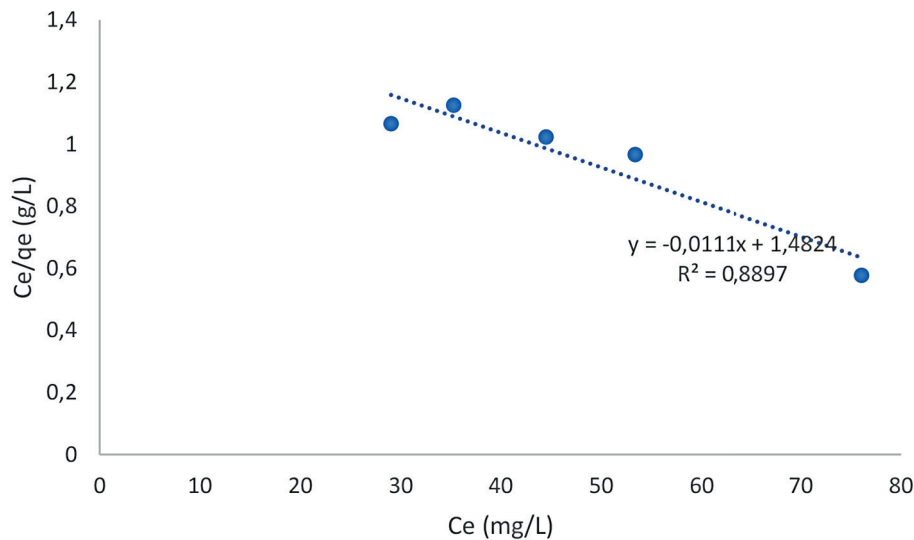


Figure 10. The adsorption isotherm plot of the Freundlich model

adsorbent. The test of the adsorption behavior of activated carbon on  $Cr^{6+}$  ions using the Freundlich and Langmuir equations is presented in Figures 10 and 11. Meanwhile, the parameters for the adsorption isotherm of  $Cr^{6+}$  ions by activated carbon are presented in Table 2.

## CONCLUSIONS

The best conditions in the process of manufacturing activated carbon from bituminous coal with ammonium phosphate reagent are at a concentration of 0.5–2 M and a temperature of 1048–1148 K.



**Figure 11.** Plotting  $C_e$  vs.  $C_e/q_e$  to obtain the Equation constant for the Langmuir type isotherm adsorption

**Table 2.** Langmuir isotherm adsorption constant of  $\text{Cr}^{6+}$  solution by activated carbon as a result of this study

Adsorption type	Freundlich isotherm			Langmuir isotherm		
Constant	$R^2$	$n$	$K_F$ (mg/g)	$R^2$	$b$ (L/mg)	$q_m$ (mg/g)
Constant value	0.5126	2.487	8.8818	0.8897	-0.0075	-90.0901

The best characteristics of activated carbon produced are water content of 0.16–0.74%, volatile matter content 14.38–19.31%, ash content 6.48–9.97%, fixed carbon content 70.60–75.79%, iodine number 1243–1259 mg/g, specific surface area 31.930 m<sup>2</sup>/g, pore surface area 8.905 m<sup>2</sup>/g, pore volume 0.011 cc/g, and pore radius 30.614. Meanwhile, activated carbon can decrease the chromium content in artificial batik waste with a maximum adsorption capacity of 52 mg/g and a removal percentage of 37–53%. Furthermore, the Freundlich equation test produced  $R^2$ ,  $n$ , and  $K_F$  constants of 0.5126, 2.4870, and 8.8818 mg/g, while the Langmuir equation test produced  $R^2$ ,  $b$ , and  $q_m$  constants of 0.8897, -0.0075 L/mg, and -90.0901 mg/g.

## REFERENCES

1. Yáñez-Varela A.J., Mendoza-Escamilla V.X., Alonzo-García A., Martínez-Delgado S.A., González-Neria I., Gutiérrez-Torres C. 2018. CFD and experimental validation of an electrochemical reactor electrode design for Cr(VI) removal. *Chemical Engineering Journal*, 349, 119–128. <https://doi.org/10.1016/j.cej.2018.05.067>
2. Budianto A., Kusdarini E., Amrullah N.H., Ningsih E., Udyani K.A. 2021. Physics and chemical activation to produce activated carbon from empty palm oil bunches waste. *IOP Conference Series: Materials Science and Engineering*. IOP Publishing.
3. Budihardjo A.M., Wibowo G.Y., Ramadan S.B., Serunting M.A., Yohana E., Syafrudin. 2021. Mercury removal using modified activated carbon of peat soil and coal in simulated landfill leachate. *Environmental Technology & Innovation*, 24. <https://doi.org/10.1016/j.eti.2021.102022>
4. Azha S.F., Ismail S. 2021. Feasible and economical treatment of real hand-drawn batik/textile effluent using zwitterionic adsorbent coating: Removal performance and industrial application approach. *Journal of Water Process Engineering*, 41, 1–12. <https://doi.org/10.1016/j.jwpe.2021.102093>
5. Basu S., Ghosh G., Saha S. 2018. Adsorption characteristics of phosphoric acid induced activation of bio-carbon: Equilibrium, kinetics, thermodynamics and batch adsorber design. *Process Safety and Environmental Protection*, 117, 125–142. <https://doi.org/10.1016/j.psep.2018.04.015>
6. BSN. 1995. Standar Nasional Indonesia untuk Karbon Aktif Teknis SNI 06-3730-1995.
7. Budianto A., Kusdarini E., Effendi S.S.W., Aziz M. 2019. The Production of Activated Carbon from Indonesian Mangrove Charcoal. *IOP Conference Series: Materials Science and Engineering*, 462(1). <https://doi.org/10.1088/1757-899X/462/1/012006>
8. Budianto A., Kusdarini E., Mangkurat W., Nurdiana E., Asri N. 2021. Activated Carbon Producing from Young Coconut Coir and Shells to Meet Activated Carbon Needs in Water Purification Process.

- Journal of Physics: Conference Series. Surabaya: IOP Publishing.
9. Budianto A., Kusdarini E., Effendi S., Aziz M. 2019. The Production of Activated Carbon from Indonesian Mangrove Charcoal. *Materials Science and Engineering*, 462, 1–8. <https://doi.org/10.1088/1757-899X/462/1/012006>
  10. Dhivya E., Magadevan D., Palguna Y., Mishra T., Aman N. 2019. Synthesis of titanium based hetero MOF photocatalyst for reduction of Cr (VI) from wastewater. *Journal of Environmental Chemical Engineering*, 7(4), 103240. <https://doi.org/https://doi.org/10.1016/j.jece.2019.103240>
  11. Effendi H. 2003. *Telaah Kualitas Air : Bagi Pengelolaan Sumber Daya dan Lingkungan Perairan*. Bogor: Kanisius, IPB.
  12. Fatimah I., Sahroni I., Dahlyani M.S.E., Oktaviyani A.M.N., Nurillahi R. 2021. Surfactant-modified *Salacca zalacca* skin as adsorbent for removal of methylene blue and Batik's wastewater. *Materials Today: Proceedings*, 44, 3211–3216. <https://doi.org/https://doi.org/10.1016/j.matpr.2020.11.440>
  13. Gong Y., Gai L., Tang J., Fu J., Wang Q., Zeng E.Y. 2017. Reduction of Cr(VI) in simulated groundwater by FeS-coated iron magnetic nanoparticles. *Science of The Total Environment*, 595, 743–751. <https://doi.org/https://doi.org/10.1016/j.scitotenv.2017.03.282>
  14. Hessley R.K., Reasoner J.E., Riley J.T. 1986. *Coal Science (Tenth Edit)*. New York: John Wiley & Sons Inc.
  15. Kirk R.E., Othmer D.F. 1979. *Encyclopedia of Chemical Technology (Third Edit)*. New York: John Wiley & Sons Inc.
  16. Kusdarini E., Budianto A. 2018. Removal of Manganese from Well-Water on Pasuruan, East Java, Indonesia Using Fixed Bed Cation Exchanger and Prediction of Kinetics Adsorption. *Indian Journal of Science and Technology*, 11(23), 1–7.
  17. Kusdarini E., Budianto A., Ghafarunnisa D. 2017. Produksi Karbon Aktif dari Batubara Bituminus dengan Aktivasi Tunggal H<sub>3</sub>PO<sub>4</sub>, Kombinasi H<sub>3</sub>PO<sub>4</sub>-NH<sub>4</sub>HCO<sub>3</sub>, dan Termal. *Reaktor*, 17(2), 74–80. <https://doi.org/http://dx.doi.org/10.14710/reaktor.17.2.74-80>
  18. Kusdarini E., Hakim L., Yanuwadi B., Suyadi S. 2021. Study in the Development of Fixed Bed Filter Adoption of Public Health of Lake Water Users. *Walailak Journal of Science and Technology*, 18(8), 1–10. <https://doi.org/https://doi.org/10.48048/wjst.2021.9131>
  19. Kusdarini E., Purwaningsih D.Y., Budianto A. 2018. Adsorption of Pb<sup>2+</sup> Ion in Water Well with Amberlite Ir 120 Na Resin. *Pollution Research*, 37(4), 307–312.
  20. Kusdarini E., Purwaningsih D.Y., Budianto A. 2021. Removal Pb<sup>2+</sup> of Well Water using Purolite C-100 Resin and Adsorption Kinetic. *Pollution Research*, 40(2).
  21. Kusdarini E., Yanuwadi B., Hakim L., Suyadi S. 2020. Adoption Model of Water Filter by The Society of Lake Water Users in Dry Land Area, Gresik, East Java, Indonesia. *International Journal on Advanced Science Engineering Information Technology*, 10(5), 2089–2096.
  22. Liu W., Jin L., Xu J., Liu J., Li Y., Zhou P., Wang X. 2019. Insight into pH dependent Cr(VI) removal with magnetic Fe<sub>3</sub>S<sub>4</sub>. *Chemical Engineering Journal*, 359, 564–571. <https://doi.org/https://doi.org/10.1016/j.ccej.2018.11.192>
  23. Liu X., Li Q., Zhang G., Zheng Y., Zhao Y. 2022. Preparation of activated carbon from Guhanshan coal and its effect on methane adsorption thermodynamics at different temperatures. *Powder Technology*, 395, 424–442. <https://doi.org/https://doi.org/10.1016/j.powtec.2021.09.076>
  24. Mahmudi M., Arsad S., Amelia M.C., Rohmaningsih H.A., Prasetya F.S. 2020. An Alternative Activated Carbon from Agricultural Waste on Chromium Removal. *Journal of Ecological Engineering*, 21(8), 1–9. <https://doi.org/https://doi.org/10.12911/22998993/127431>
  25. Fu M.M., Mo C.H., Li H., Zhang Y.N., Huang W.X., Wong M.H. 2019. Comparison of physicochemical properties of biochars and hydrochars produced from food wastes. *Journal of Cleaner Production*, 236. <https://doi.org/https://doi.org/10.1016/j.jclepro.2019.117637>
  26. Nowruzi R., Heydari M., Javanbakht V. 2020. Synthesis of a chitosan/polyvinyl alcohol/activate carbon biocomposite for removal of hexavalent chromium from aqueous solution. *International Journal of Biological Macromolecules*, 147, 209–216.
  27. Song G., Deng R., Yao Z., Chen H., Romero C., Lowe T., Baltrusaitis J. 2020. Anthracite coal-based activated carbon for elemental Hg adsorption in T simulated flue gas: Preparation and evaluation. *Fuel*, 275, 1–10. <https://doi.org/https://doi.org/10.1016/j.fuel.2020.117921>
  28. Suliestyah, Astuti A.D. 2021. Optimasi Aktivator ZnCl<sub>2</sub> dalam Pembuatan Karbon Aktif dari Batubara dan Pengujian Karbon Aktif sebagai Adsorben. *Penelitian Dan Karya Ilmiah*, 6(2), 191–201.
  29. Wirosedarmo R., Anugroho F., Mustaqiman A.N., Amanah R., Gustinasari K. 2020. Phytore-mediation of chrome in batik industry wastewater using *Cyperus haspan*. *Nanotechnology for Envi-Ronmental Engineering*, 5(2), 1–7.